

## Article

# Assessment of the Effect of Thermal-Assisted Machining on the Machinability of SKD11 Alloy Steel

Thi-Bich Mac <sup>1</sup>, The-Thanh Luyen <sup>1</sup> and Duc-Toan Nguyen <sup>2,\*</sup><sup>1</sup> Faculty of Mechanical Engineering, Hungyen University of Technology and Education, Hungyen 100000, Vietnam<sup>2</sup> School of Mechanical Engineering, Hanoi University of Science and Technology, 1A-Dai Co Viet Street, Hai Ba Trung District, Hanoi City 100000, Vietnam

\* Correspondence: toan.nguyenduc@hust.edu.vn; Tel.: +84-43-869-2007

**Abstract:** This study aimed to investigate the effects of Thermal-Assisted Machining (TAM) on SKD11 alloy steel using titanium-coated hard-alloy insert cutting tools. The microstructure, material hardness, chip color, cutting force, chip shrinkage coefficient, roughness, and vibration during TAM were evaluated under uniform cutting conditions. The machining process was monitored using advanced equipment. The results indicated that thermal-assisted processing up to 400 °C did not alter the microstructure and hardness of the SKD11 alloy steel. However, a significant variation in chip color was observed, indicating improved heat transfer through TAM. The cutting force, vibration amplitude of the workpiece, and surface roughness all decreased with increasing TAM. Conversely, the chip shrinkage coefficient of the machined chips tended to increase due to the high temperatures.

**Keywords:** SKD11 alloy steel; machinability; thermal-assisted machining (TAM)



**Citation:** Mac, T.-B.; Luyen, T.-T.; Nguyen, D.-T. Assessment of the Effect of Thermal-Assisted Machining on the Machinability of SKD11 Alloy Steel. *Metals* **2023**, *13*, 699. <https://doi.org/10.3390/met13040699>

Academic Editors: George A. Pantazopoulos and Badis Haddad

Received: 17 February 2023

Revised: 27 March 2023

Accepted: 31 March 2023

Published: 3 April 2023



**Copyright:** © 2023 by the authors. Licensee MDPI, Basel, Switzerland. This article is an open access article distributed under the terms and conditions of the Creative Commons Attribution (CC BY) license (<https://creativecommons.org/licenses/by/4.0/>).

## 1. Introduction

The cutting mode and tool geometry parameters play a critical role in machining techniques, especially when working with materials that are challenging to machine due to their high hardness. These parameters affect various output parameters of the machining process, such as cutting force, cutting heat, cutting tool wear, cutting process vibration, surface roughness, and chip geometry. To improve productivity, part quality, and cost-effectiveness, researchers are constantly seeking new technological solutions to support the machining process, including the use of smooth cold techniques, new cutting tool materials, vibration-assisted cutting, and thermal-assisted machining. Difficult-to-machine materials, characterized by high hardness, good wear resistance, and little change in mechanical properties at high temperatures, are widely used in various industries, such as mechanical, automotive, aerospace, aviation, defense, medical, and electrical-electronics-automation. Surveys have shown that over 30% of milling, turning, and drilling operations are performed on such materials [1].

Thermal-assisted machining (TAM) is a machining process that involves heating the workpiece before machining it using traditional or CNC machines. This technique has been extensively used in industrial production since its introduction in 1945 [1,2]. Compared to traditional machining methods, TAM offers several advantages, such as increased tool life, reduced cutting force, decreased tool wear, and improved surface quality, resulting in enhanced productivity [3–5]. TAM is suitable for both cutting processes (e.g., turning, milling, drilling) and deformation processes (e.g., forging, stamping, drawing). Several heating methods can be employed for TAM, including electrical current heating, laser beam heating (LAM), plasma heating (PEM), furnace heating (FAM), and induction heating (IAM). While each method has its own benefits and drawbacks, induction heating (IAM) is particularly effective due to its high heating capacity, ease of use, and affordability, making it a great choice for metalworking operations [6].

Many studies have suggested eco-friendly dry and minimum quantity lubrication or optimization to improve machining productivity, increase tool life, and enhance product quality [7–9]. However, for challenging-to-machine materials, like those commonly used in heavy-duty industries such as automotive, marine, and aviation, advanced machining methods such as diamond grinding or discharge machining are often used but limited by low material removal rates, expensive tools, and rapid wear [2]. Among these materials, SKD11 Tool Steel is frequently utilized in mold and automotive sectors due to its hardness, strength, and ductility [10]. Although traditional techniques like diamond grinding or discharge machining are limited by high costs and specialized technologies, TAM has been introduced as an innovative solution to the challenges of machining SKD11. Studies have indicated that machining with TAM can reduce cutting forces by up to 40%, increase tool life, enhance surface roughness by up to 50%, and increase material removal rate when compared to machining at room temperature [11–13].

Recent research has shown that using thermal-assisted machining (TAM) can offer several advantages, including improved tool life, enhanced productivity, and better working conditions between the tool and workpiece [14–16]. Studies have revealed that workpiece temperature is directly proportional to tool life and inversely proportional to cutting speed. Induction heating has been investigated for milling titanium alloy Ti-6Al-4V, with heat treatment significantly improving tool life and material removal rate, by up to 169.4% at a temperature of 650 °C. However, heating above 640 °C may negatively impact the workpiece's mechanical properties, reducing machining efficiency [5,17]. Studies have also shown that cutting and shear forces are inversely proportional to temperature, with a 13% reduction in cutting force observed when machining at 500 °C compared to room temperature. A novel approach to machining Inconel 718 was presented by Wang et al. [18], which combines traditional turning, cryogenic enhanced machining, and plasma heating. Cold working techniques can reduce the heat generated during cutting, enhancing the cutting tool's longevity. The implementation of this method has been shown to result in a substantial enhancement of the machining process, with the surface gloss of the machined material increased by a factor of 2.5, the required machining force decreased by half, and the cutting tool's lifespan prolonged by a factor of 1.7 compared to traditional machining at room temperature.

Efficiently machining hard alloys has long been a challenge, but thermally assisted machining (TAM) offers a promising solution. TAM involves cutting the material and then softening it with an external heat source, which has been shown to reduce the hardness and tensile strength of the workpiece material, thereby improving machinability [19]. Research indicates that TAM is linked to higher material removal rates, better control of machining time, and improved surface finishes. TAM is particularly advantageous for machining bio-implant titanium alloys, which require high precision. Hard steels can also be successfully machined using TAM, resulting in lower cutting forces, increased tool life, and higher material removal rates [20–24]. TAM can reduce cutting force amplitudes and chip morphology changes, resulting in less vibration and better surface integrity. However, machining certain hardenable steels, such as 1090 steel, can lead to increased cutting forces due to phase transformation hardening when the laser-preheated part enters the cutting zone. Softening the workpiece by reaching surface temperatures of 300–400 °C for an uncut chip thickness of 0.05 mm, on the other hand, can reduce the magnitude and amplitude variation of cutting forces, and limit the evolution of tool wear [25]. TAM also induces a change in chip morphology from sawtooth to continuous, improving the surface finish. While TAM can lead to higher cutting forces in some hardenable steels, it can also enhance surface integrity [26].

TAM techniques have been extensively researched and used in production. However, little is known about the use of magnetic induction heating for mold steel, particularly when milling difficult materials like SKD11 steel, which is commonly used in industry. This study aims to evaluate the influence of TAM on milling SKD11 steel and its effect on the material's machinability by analyzing cutting force, vibration amplitude of the workpiece, and surface

roughness. This analysis provides a basis for selecting appropriate TAM process parameters. A significant challenge when using electromagnetic induction heating in machining is its application to large parts with varying sizes or complex shapes. This study proposes a potential technological solution for processing difficult materials using electromagnetic induction heating. The results demonstrate that the heating process effectively reduces cutting force, cutting heat, and vibration during cutting, while improving the surface quality of the workpieces. The findings of this study have practical implications and are applicable to the manufacturing industry.

## 2. Experimental Setup

The ease or difficulty of processing a material is known as its machinability, which can be evaluated using parameters such as tool life, MRR, cutting force, cutting process vibration, and surface gloss of the machined material. The machinability of a material is greatly affected by its microstructure, which can be further influenced by the cutting mode. Therefore, it is essential to assess the machinability of materials during heating processing and compare it to conventional machining to determine the impact of heating on the machinability of SKD11 steel materials.

### 2.1. Schematic of Experimental System

This study establishes an experimental research model that is based on the research objectives and the available experimental equipment, as depicted in Figure 2.

### 2.2. Materials and Testing Equipment

SKD11 steel is a frequently used alloy steel in mold processing, as defined by JIS-G4404. This steel is notable for its hardness, strength, and ductility, and can maintain its hardness even at high temperatures for an extended period, making it suitable for use in the production of molds for extrusion, plastic injection, pressure, and components that require specific performance characteristics. Table 1 presents a breakdown of the SKD11 steel components, expressed as a weight percentage (wt%).

**Table 1.** The chemical composition of SKD11 steel (wt%) [27].

C	Cr	Mo	Si	Mn	Ni	V
1.4–1.6	11–13	0.7–1.2	≤0.6	≤0.6	-	0.15–0.3

In this study, a machining experiment was conducted on SKD11 steel test specimens using a Taiwanese MC500 milling machine. The billet was rough-worked and had dimensions of  $70 \times 31 \times 80 \text{ mm}^3$ , and a chamfer of  $7 \text{ mm} \times 7 \text{ mm}$  was applied for uniform contact with the induction coil. For the milling process, a 40 mm face milling cutter was used, equipped with a titanium-coated hard alloy insert manufactured by PRAMET, a tool manufacturer from the Czech Republic. Specifically, the APKT 1604PDR–GM hard alloy piece was utilized, with cutting edge parameters such as the rake angle, clearance angle, and cutting-edge radius set at  $24^\circ$ ,  $11^\circ$ , and 0.8 mm, respectively. Other geometric parameters, including  $l = 16 \text{ mm}$ ,  $d = 9.44 \text{ mm}$ ,  $s = 5.67 \text{ mm}$ , and  $d_1 = 4.6 \text{ mm}$ , were also specified. No coolant was applied during the machining process. One significant challenge in this research was the application of electromagnetic induction heating in machining, as depicted in Figure 1d.

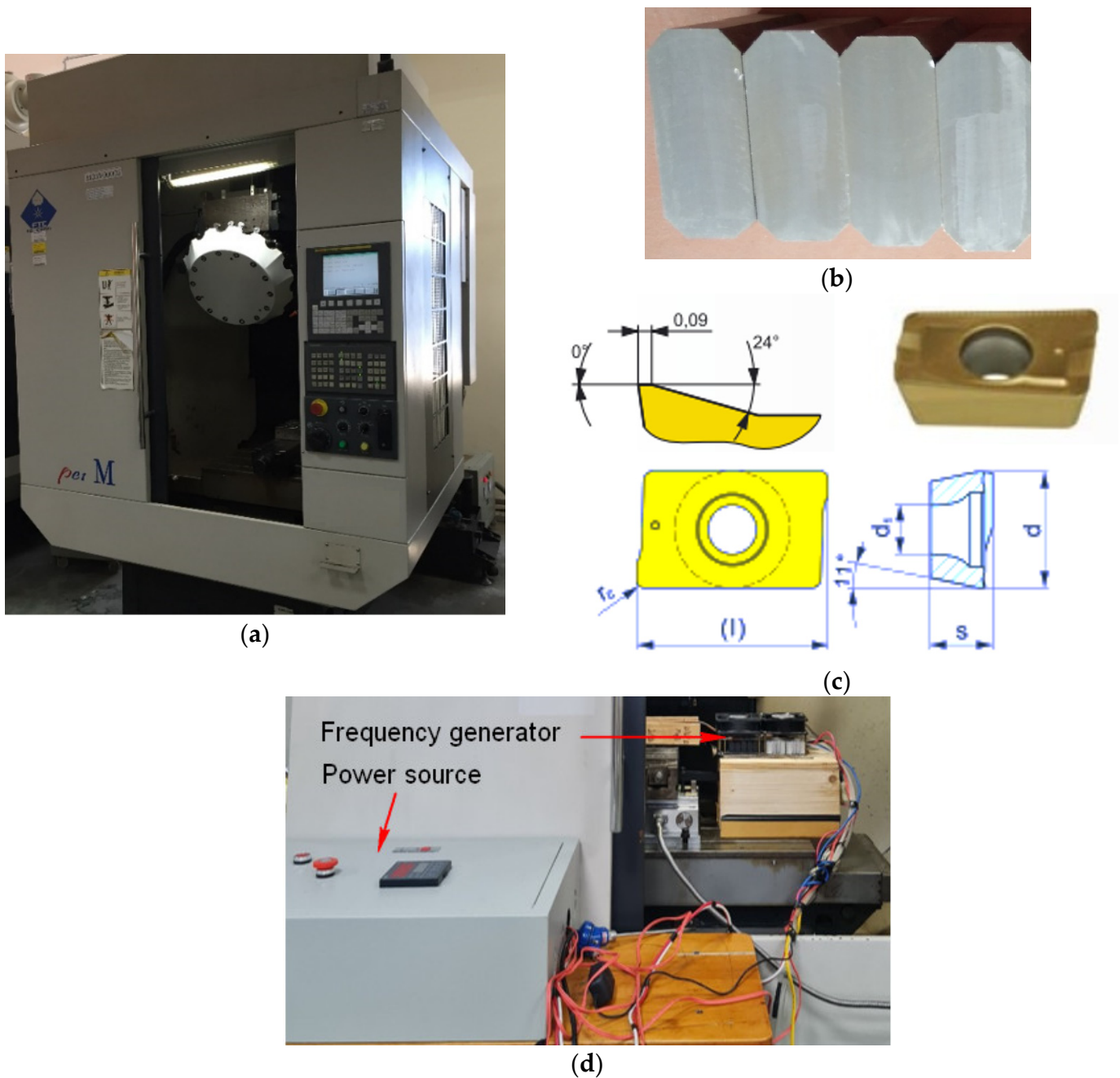
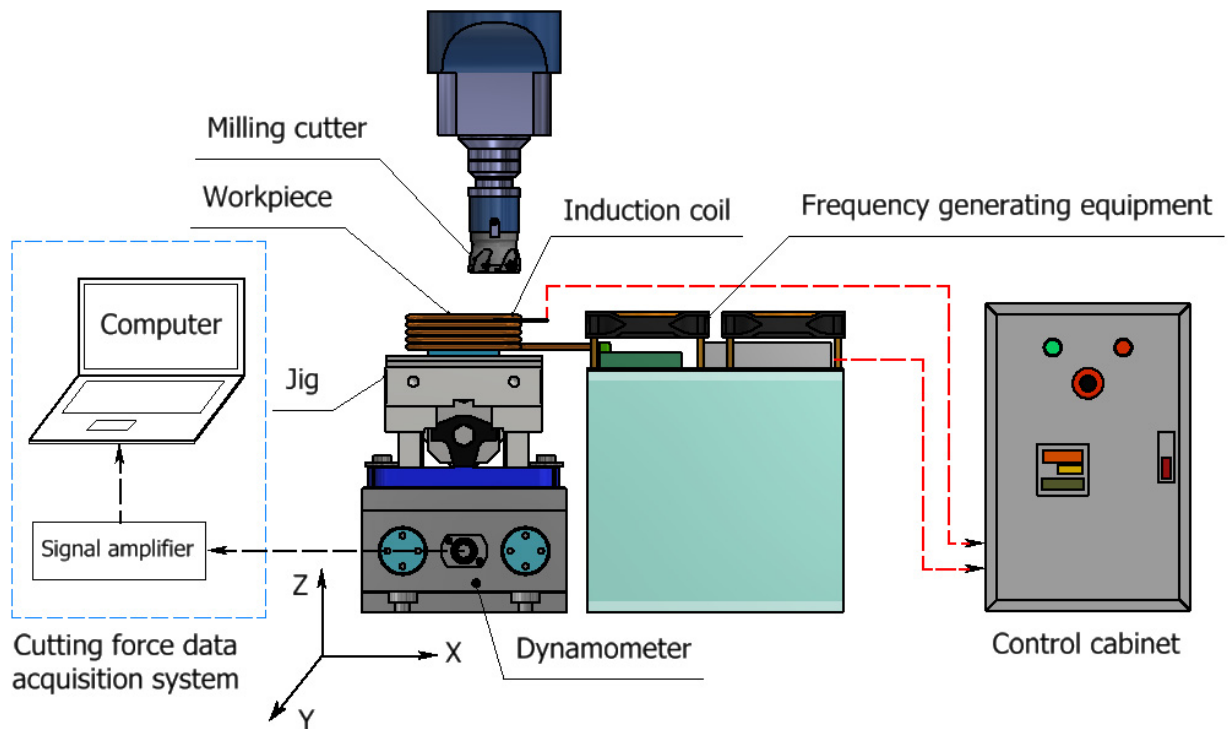
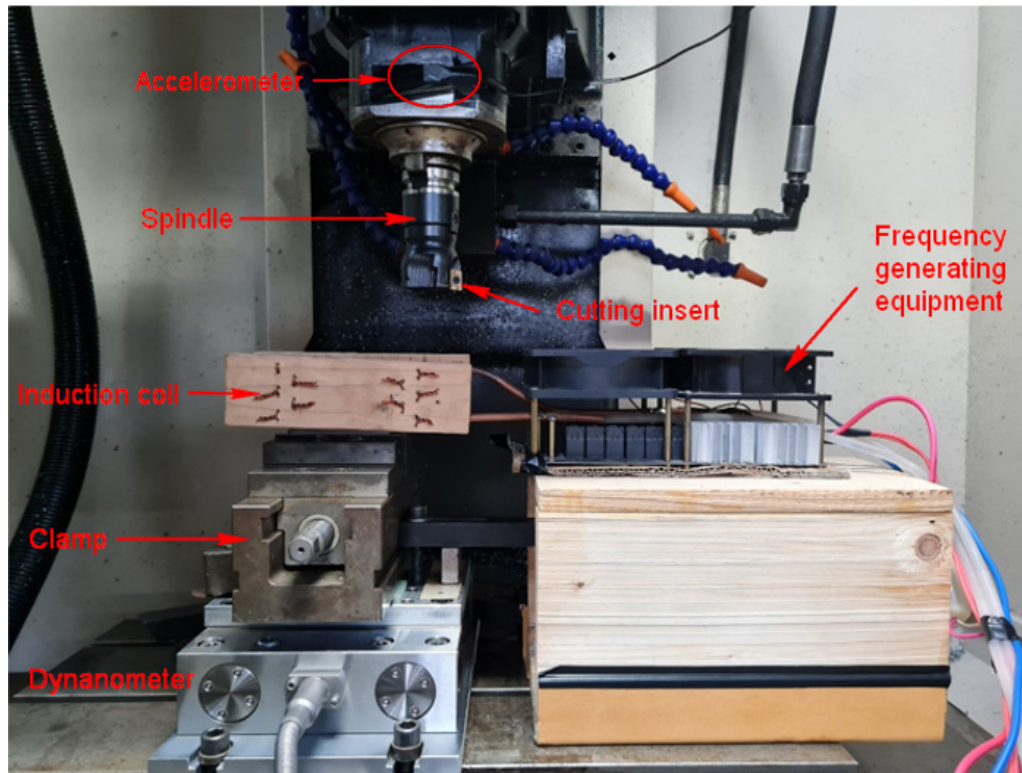


**Figure 1.** Components of the experimental system. (a) MC500 Milling Machine, (b) Sample Workpieces, (c) Hard Alloy Insert, and (d) Power Source-Frequency Generator.

The study utilized the Axiovert 25 CA optical microscope (Figure 3a) to examine the microstructure of the material after heating at different temperatures and compare it with the original sample. This microscope, specifically designed for materials research, is used in conjunction with Image-Pro Plus image analysis software to analyze the material phase. The study also employed the Brinell hardness tester (Figure 3b) to test the initial and post-heating samples for hardness.



(a)



(b)

**Figure 2.** Schematic of Experimental System. Schematic diagram (a) and experiment photograph in working zone (b).

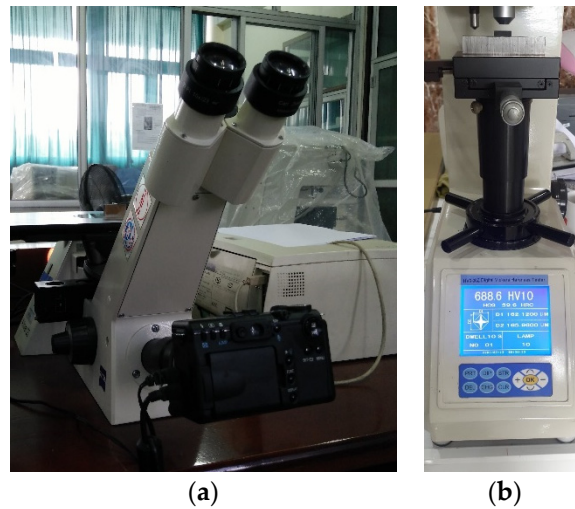


**Figure 3.** Equipment used in the tests: (a) Axiovert 25 CA Optical Microscope, (b) Brinell Hardness Tester.

### 3. SKD11 Steel Material Machinability Results

#### 3.1. Effect of TAM on Microstructure of SKD11 Steel

To conduct an accurate examination of the microscopic structure of materials, proper sample preparation is crucial. The process of preparing metal samples involves multiple stages, including cutting, grinding, polishing, and impregnation. Specimens are initially machined following established standards to achieve a size that can be impregnated. Figure 4 displays the experimental samples and their cross-sections for SEM examination.

Figure 4 illustrates the microstructural analysis of SKD11 alloy steel samples before and after thermal-assisted machining (TAM) at different temperatures, using optical microscopy. Figure 4a presents an image of the microstructure of the original material sample, while Figure 4b–d show images of the microstructure after TAM at different temperatures. The analysis reveals that the microstructure of the samples after TAM at room temperature and 400 °C is similar to that of the original material. Specifically, the microstructure of the four samples includes white plates and bright round particles of chromium Cr<sub>7</sub>C<sub>3</sub> carbides, spherical dark dots of Cementite, and a light background of Pearlite. These observations suggest that the microstructure of the specimen remains unchanged even when the temperature is increased to 400 °C, which is below the phase transition temperature of 700 °C for the SKD11 alloy steel [28].

#### 3.2. Effect of TAM on Hardness

To evaluate the impact of elevated temperatures on workpiece hardness after heating, the workpiece was exposed to the designated temperature and allowed to cool naturally via exposure to ambient air. Surface hardness measurements necessitated meticulous sample preparation, including cutting, grinding, polishing, and impregnation. In order to prevent the influence of cutting heat, wire cutters were employed during sample cutting. The grinding process aimed to minimize undulation caused by the varying hardness of structural elements, while polishing removed any coarse grinding marks and scratches. Finally, deformations from the cutting, grinding, and polishing stages were either eliminated or leveled to a size sufficient for removal with an impregnating agent. Three hardness measurements were taken on each sample using a Brinell hardness tester at distinct locations, as illustrated in Figure 5. The results, presented in Figure 5, showed that increasing temperatures resulted in decreased specimen hardness to 2–3 HB at 200 °C and 300 °C. However, at 400 °C the sample demonstrated increased hardness compared to the other temperatures, although this increase was not significant within the chosen experimental temperature range.

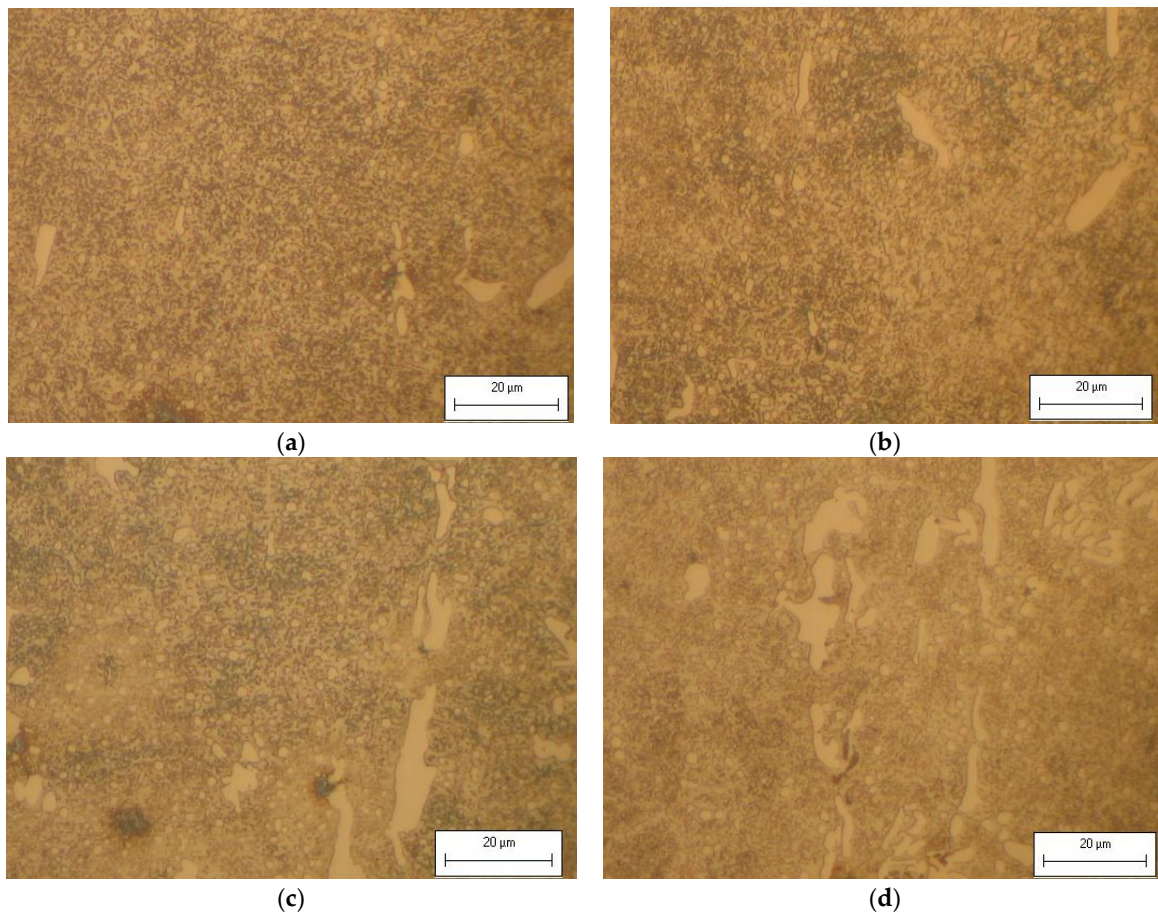


**Figure 4.** Microstructure of Material Samples at Different Temperatures: (a) Room Temperature, (b) 200 °C, (c) 300 °C, and (d) 400 °C.

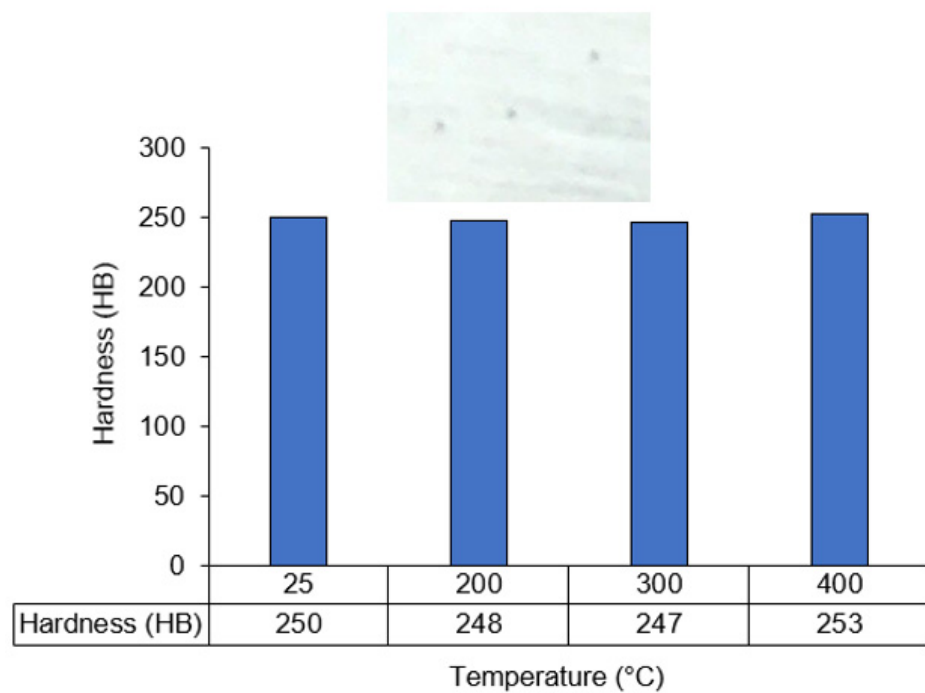


**Figure 5.** Workpiece hardness after heating at different temperatures and natural air-cooling.

### 3.3. Effect of TAM on Chip Color

The geometry and morphology of chips play a crucial role in assessing the machinability of materials. Chip geometry affects cutting force, cutting heat, and tool wear, while chip morphology provides valuable insights for milling tool design. Therefore, when analyzing the impact of heating on the machinability of SKD11, examining chip formation is crucial. Figure 6 shows chip images obtained during the milling of SKD11 steel under different cutting modes and heating conditions. Figure 6a–d display chip formations during machining at various temperatures. The formation of wire chips is due to the workpiece material's ductile properties. The chip color varies significantly, with the normal machining chip appearing purple-black in color due to excessive cutting heat generated during machining at room temperature (Figure 6a). In contrast, chips appear bright white (Figure 6b) and yellow (Figure 6c) when machined at 200 °C and 300 °C, respectively. The chip appears darker yellow when machined at 400 °C (Figure 6d). This variation can be attributed to the uniform transfer of heat between the cutting tool, workpiece, and chip during heating processing. The high temperature reduces the material's tensile strength, mechanical strength, and yield stress, while increasing its deformation, improving heat transfer conditions, and decreasing the bonding force between metal molecules [19,20]. As a result, chip removal becomes easier, cutting heat is reduced, and chips appear light-colored during hot machining. The results suggest that temperatures between 200–300 °C preserve the chip color compared to the original substrate material.

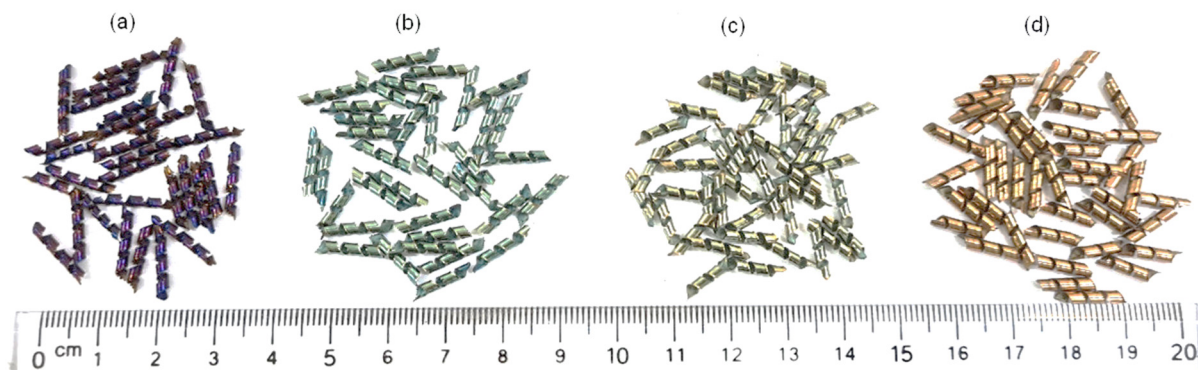


**Figure 6.** Chip Formation at Different Temperatures: (a) Room Temperature, (b) 200 °C, (c) 300 °C and (d) 400 °C.

### 3.4. Effect of TAM on Cutting Force

An experimental study was conducted to investigate the effect of elevated temperature on cutting forces ( $F$ ) during milling with identical cutting parameters at room temperature and elevated temperature. The cutting force is a dynamic phenomenon and changes throughout the machining cycle [29]. Figure 7 displays the cutting force transformation with respect to tool distance during milling at room temperature (25 °C) and elevated temperature (200 °C). The cutting parameters used were a cutting speed of 235 m/min, feed rate of 305 mm/min, and cutting depth of 1.5 mm. The average cutting force ( $F$ ) was calculated from the component cutting forces ( $F_f$ ,  $F_p$ ,  $F_c$ ) using Equation (1). Table 2 shows the component cutting force values and the average cutting force under conventional machining and elevated temperature conditions. The results indicate that the  $F_p$  component cutting force (direct force) has the largest value, while the radial force ( $F_f$ ) and axial force ( $F_c$ ) have relatively smaller values. The average cutting force reduction at elevated temperature compared to conventional machining is 37.5%, as determined by Equation (2)).

$$F = \sqrt{F_f^2 + F_p^2 + F_c^2} \quad (1)$$

$$\Delta F(\%) = \frac{F_T - F_R}{F_R} \times 100\% \quad (2)$$

where  $F_T$  represents the cutting force during heating and  $F_R$  represents the cutting force when machining at room temperature ( $T = 25\text{ }^\circ\text{C}$ ).

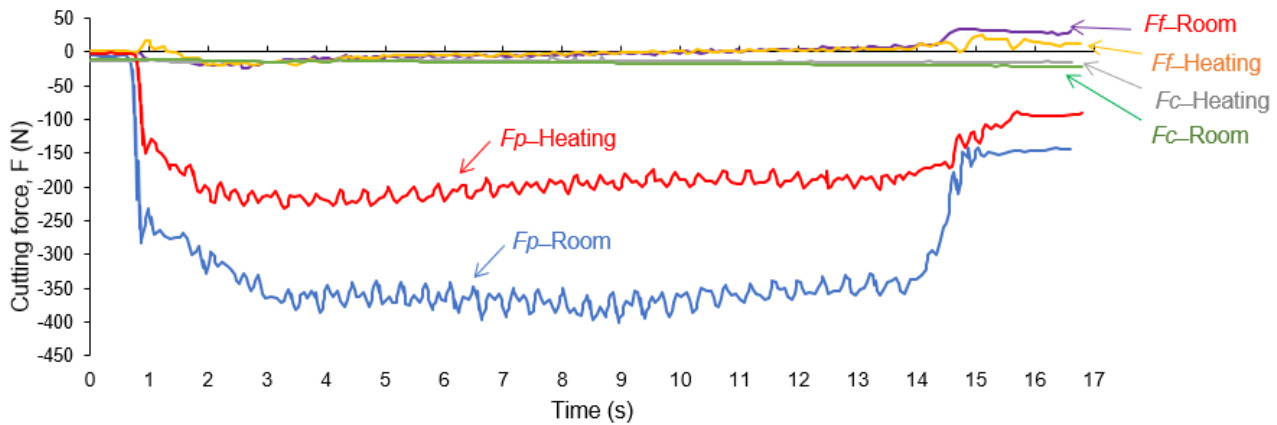


**Figure 7.** Cutting force during machining at room temperature and at elevated temperature ( $200\text{ }^\circ\text{C}$ ).

**Table 2.** Average cutting force at room and elevated temperature.

Temperature	$F_f$ (N)	$F_p$ (N)	$F_c$ (N)	$F$ (N)
Room	4.317	360.031	9.028	360.170
$200\text{ }^\circ\text{C}$	8.958	214.583	9.071	214.962

The experimental results (shown in Figure 8) indicate a significant reduction in cutting force ( $F$ ) during machining at  $200\text{ }^\circ\text{C}$  compared to conventional machining. As the heating temperature increased to  $300\text{--}400\text{ }^\circ\text{C}$ , the cutting force decreased at a slower rate. The maximum reduction in cutting force ( $\Delta F$ ) was  $65.1\%$  during milling at  $400\text{ }^\circ\text{C}$ . This reduction can be attributed to the weakening of the strength and bonding between metal molecules due to the heating process, making the cutting process easier. Moreover, in the second strain region, the compressive stress was found to decrease during heating, which led to a decrease in cutting force.

### 3.5. Effect of TAM on Surface Roughness ( $R_a$ )

The surface quality of a workpiece is critical and influenced by various factors, including the machining method, cutting tool geometry, and machining environment. Surface roughness, in particular, is essential in determining the workability and performance of the final product. This study used the average deviation criterion  $R_a$  to evaluate surface roughness. According to ISO standards,  $R_a$  is the arithmetic average of the absolute values of the profile over the reference length range ( $L = 250\text{ }\mu\text{m}$ ) for machined surfaces with a smoothness level of 8–11. The research investigated the effect of elevated temperatures on  $R_a$  during Thermal Assisted Machining (TAM) while maintaining the same cutting parameters, including speed, feed rate, and cutting depth, under various temperature conditions. The method of surface roughness measurement is shown in Figure 9a, where the measuring head moves perpendicularly to the machining trace, and each sample is measured at three locations (1, 2, 3) to ensure reliability, within the reference length range of  $250\text{ }\mu\text{m}$ , as shown in Figure 9b,c. Results indicated that heating the workpiece before machining significantly reduced surface roughness compared to conventional machining.

This is because the thermal softening of the material results in increased smoothness and stability during the cutting process.

$$\Delta Ra(\%) = \frac{Ra_R - Ra_T}{Ra_R} \times 100\% \tag{3}$$

where  $Ra_R$  and  $Ra_T$  represent the surface quality (Ra) at room and high temperature, respectively.

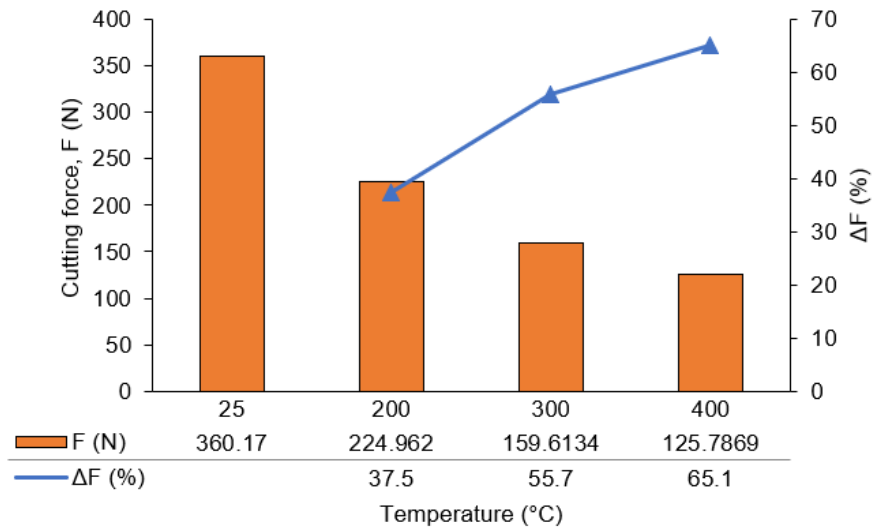


**Figure 8.** The mean cutting forces and the corresponding reductions observed during machining at various temperatures.

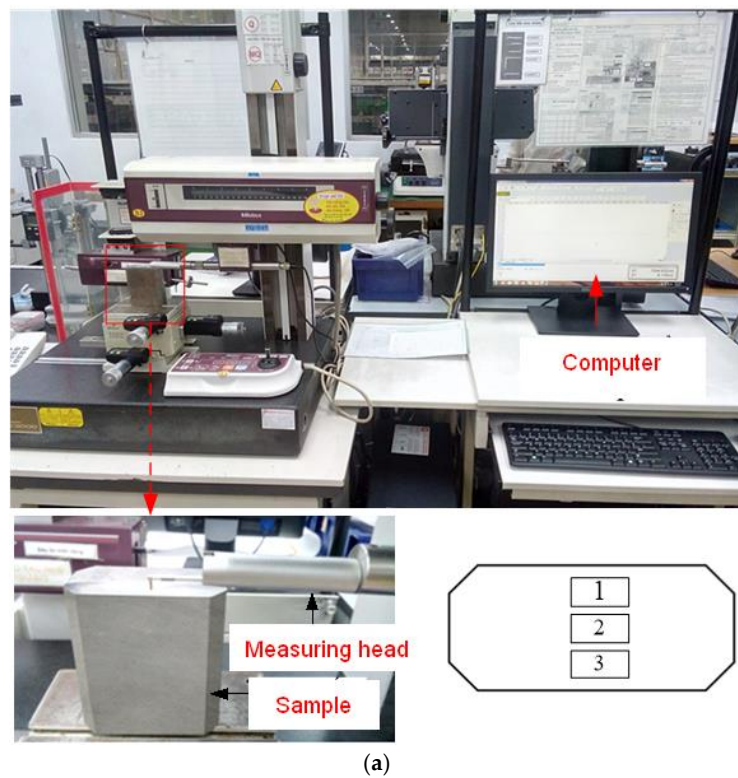


**Figure 9.** Cont.

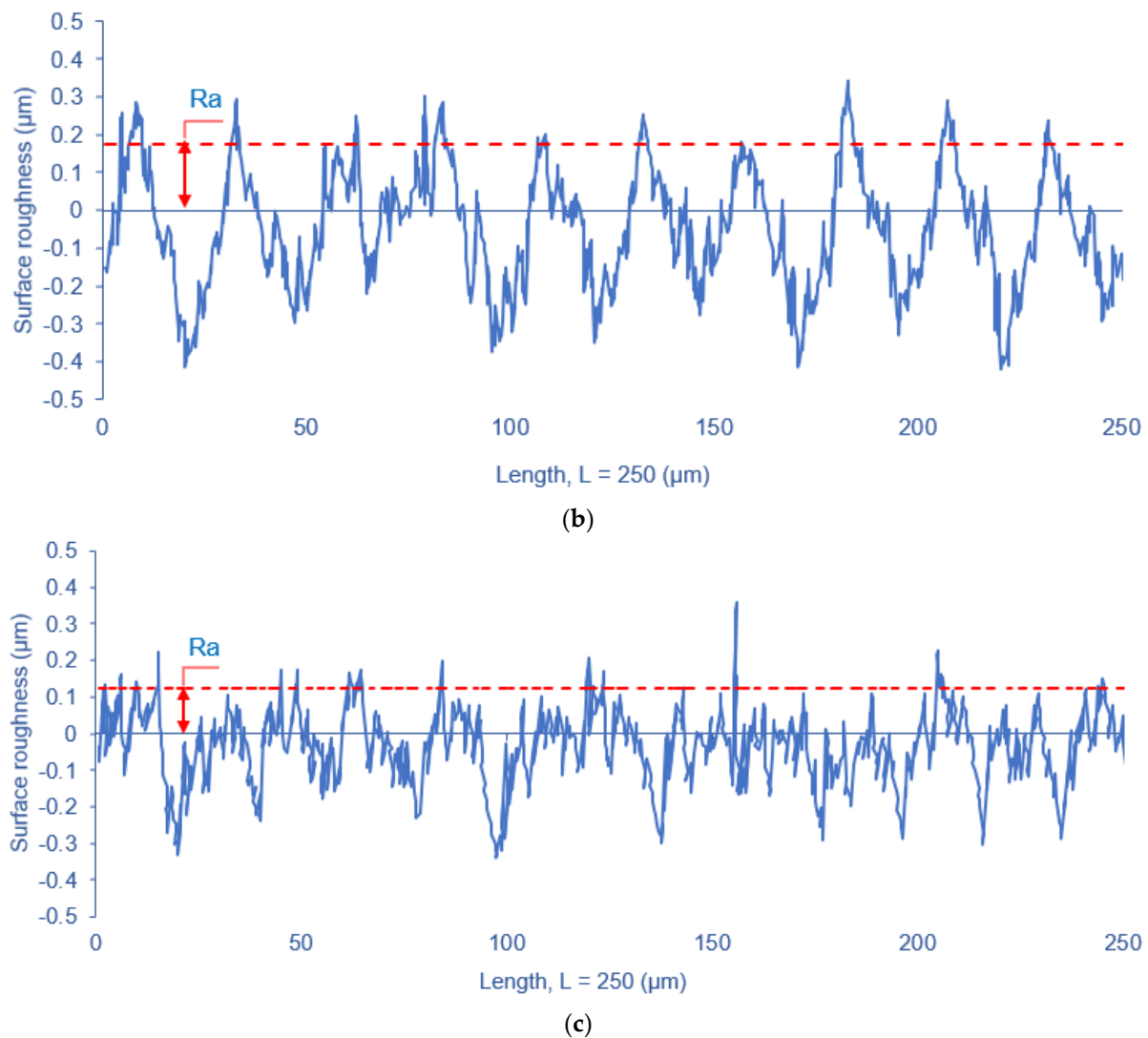


**Figure 9.** Measurement of Surface Roughness with Equipment and Method (a) and Comparison of Surface Roughness Profiles for Machining at Room Temperature (b) and 200 °C (c).

In Figure 10, the average Ra values for machining at various temperatures are plotted. The decrease in Ra was calculated using Equation (3). The results indicate that there is an inverse relationship between Ra and workpiece temperature. The greatest reduction in roughness, 47.1%, was observed at 400 °C.

### 3.6. Effect of TAM on Cutting Vibration

To investigate the impact of temperature-assisted machining (TAM) on vibration, experiments were conducted using the same cutting parameters of  $V$ ,  $f$ , and  $t$  at 235 m/min, 305 mm/min, and 1.5 mm, respectively, but at various temperature conditions. The vibration amplitudes in directions of (X, Y) as ( $A_X$  and  $A_Y$ ) were summed to obtain the  $A_{XY}$  using Equation (4).

$$A_{XY} = \sqrt{A_X^2 + A_Y^2} \quad (4)$$

Figure 11 displays the vibration amplitudes at room temperature (a) and at 200 °C (b) in directions of (X, Y). The analysis of the no-load and individual vibration data did not indicate any resonance. The results showed that TAM reduced the vibration amplitude compared to conventional machining. The reduction in cutting vibration amplitude ( $\Delta A_{XY}$ )

during TAM, as compared to milling at room temperature, is calculated using Equation (5).

$$\Delta A_{XY}(\%) = \frac{A_{XY-R} - A_{XY-T}}{A_{XY-R}} \times 100\% \tag{5}$$

where  $A_{XY-R}$ ,  $A_{XY-T}$  represent the vibration amplitudes in directions of (X, Y) during machining at room and high temperature, respectively.

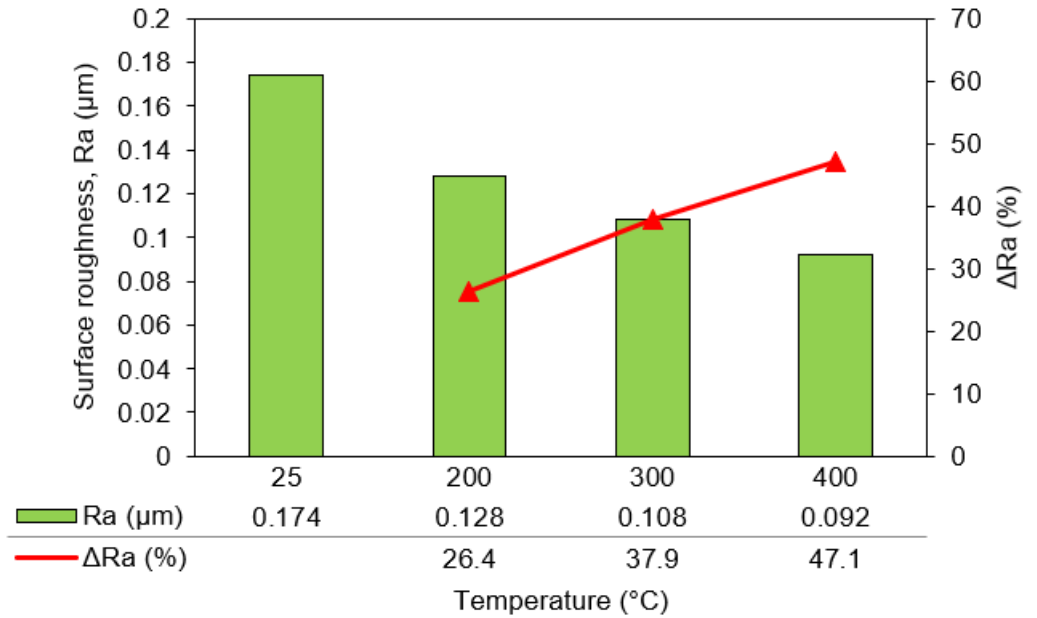


Figure 10. Surface Roughness and Reduction at Elevated Machining Temperatures.

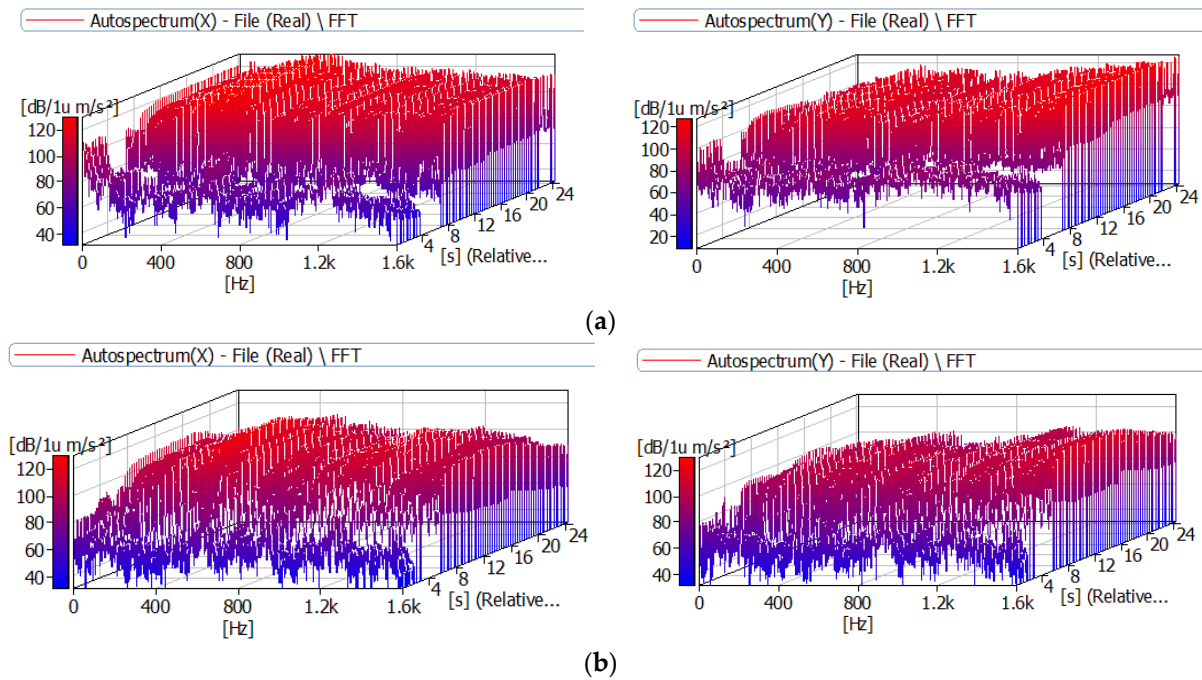
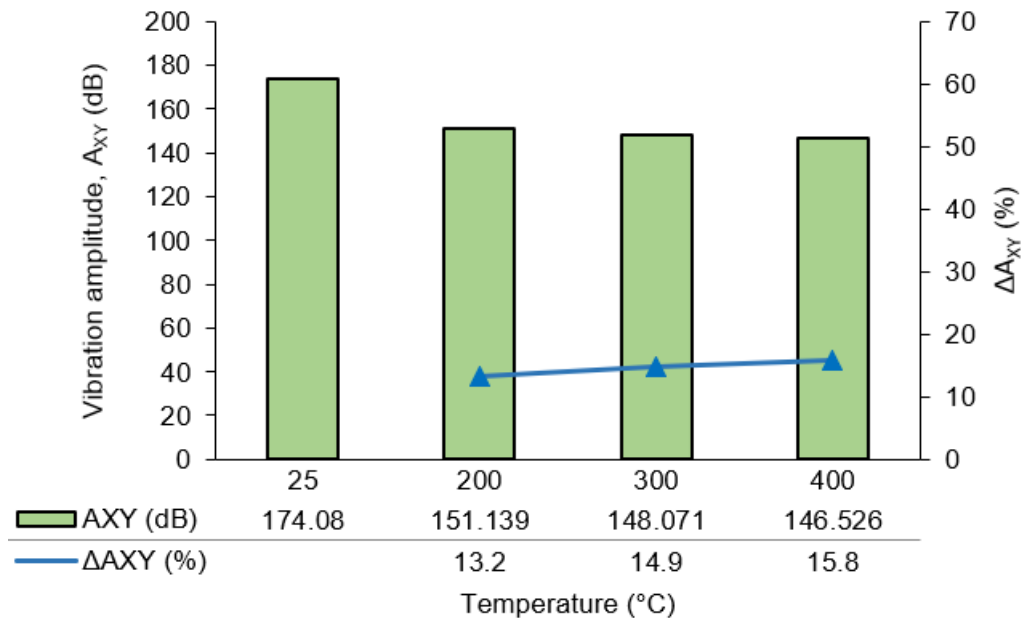


Figure 11. The vibration results at room (a) and heating at 200 °C (b) in the X and Y directions.

Figure 12 illustrates the vibration amplitude and reduction in vibration amplitude during SKD11 steel machining at various temperatures, as compared to milling at room temperature. The results indicated that  $A_{XY}$  decreased by 13.2% at 200 °C, 14.9% at

300 °C, and 15.8% at 400 °C. These findings indicate increased stability during SKD11 steel processing when conducted at higher temperatures, due to the reduction in metallic bond strength resulting in an easier cutting process. However, the reduction in vibration amplitude did not exhibit a significant change when high temperature was used to facilitate the cutting process.



**Figure 12.** Vibration amplitude and vibration amplitude reduction during machining at various temperature conditions.

### 3.7. Effect of TAM on Chip Shrinkage Coefficient ( $K$ )

$K$  is a vital parameter used to assess the plastic strain of a material during machining, and it has a significant influence on the dimensional accuracy of the machined surface. Several factors affect  $K$ , including the mechanical properties of the workpiece material, cutting tool geometry, cutting mode, and other cutting conditions. This study aims to analyze the impact of elevated temperatures on  $K$  and compare it to conventional machining under the same cutting mode. The objective is to assess the material's softening and formability at high-temperature conditions. The chip shrinkage coefficient, computed using Equation (6), is utilized to determine  $K$ .

$$K = \frac{1000 \cdot Q}{\rho \cdot L_f \cdot f \cdot t} \quad (6)$$

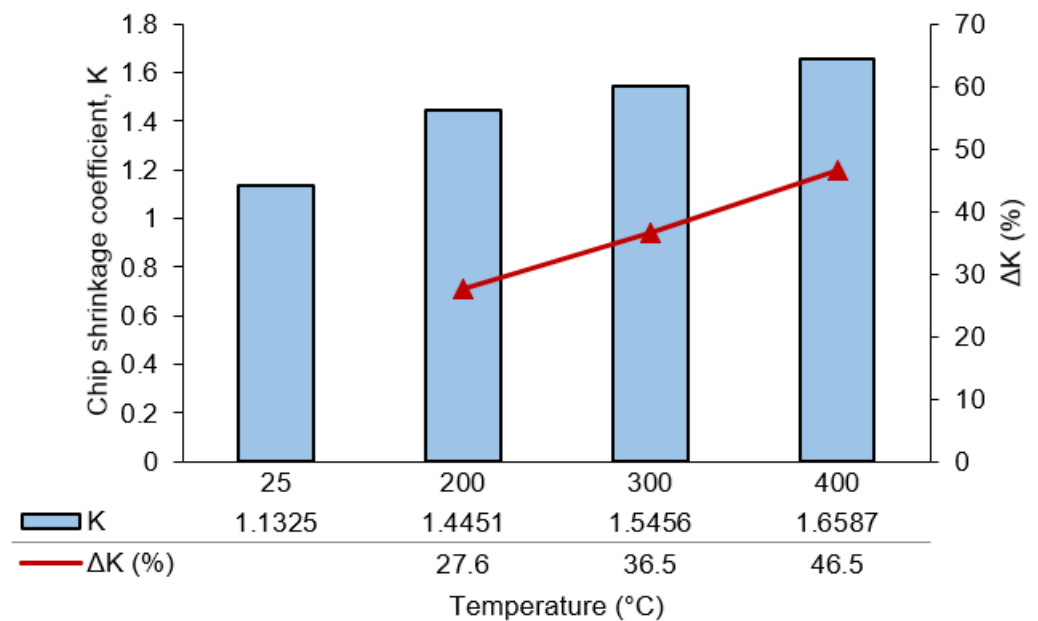
where  $Q$  and  $\rho$  represent the mass of chip (g) and the material density ( $\text{g}/\text{cm}^3$ ), respectively,  $L_f$  is the chip cutting length (mm), and  $f$  and  $t$  are the feed rate (mm/rev) and cutting depth (mm), respectively.

Figure 13 displays the chip shrinkage coefficient at different temperatures for the machining process conducted at cutting parameters of  $V = 235$  m/min,  $f = 305$  mm/min, and  $t = 1.5$  mm. The results demonstrate that the chip shrinkage coefficient increases with heating compared to conventional machining at room temperature. The increase in  $K$ , denoted as  $\Delta K$ , is calculated using Formula (7). The chip shrinkage coefficient experiences a 27.6% increase when the workpiece is heated to 200 °C, and the maximum increase in  $K$  of 46.5% is observed at a temperature of 400 °C. This trend suggests that an increase in temperature enhances the cutting process by improving the chip shrinkage coefficient. The observed phenomenon can be attributed to the material softening under high temperatures,

resulting in weakened atomic bonds and increased metal deformation, leading to a higher chip shrinkage coefficient.

$$\Delta K(\%) = \frac{K_T - K_R}{K_R} \times 100\% \quad (7)$$

where  $K_T$  and  $K_R$  represent the chip shrinkage coefficient during heating and at room temperature ( $T = 25\text{ }^\circ\text{C}$ ), respectively.



**Figure 13.** Chip shrinkage coefficient and chip shrinkage increase during machining at various temperatures.

#### 4. Conclusions

The aim of this study was to investigate and compare the effectiveness of using electromagnetic induction heating versus conventional methods for machining SKD11 steel, a material that is difficult to cut. The study analyzed various output parameters, including chip geometry, chip shrinkage coefficient, vibration amplitude, surface roughness, and cutting force. Experimental results indicated that the TAM process did not alter the material's microscopic structure in the temperature range of 200 °C to 400 °C, and the machined workpiece, cooled in air, maintained its original hardness. Additionally, the chip geometry changed and cutting force significantly decreased, with a maximum reduction of 65.1%. The  $K$  value increased by 31.7%, while surface roughness decreased notably, with a maximum reduction of 47.1% at 400 °C. Lower vibration amplitude also indicated a more stable machining process compared to traditional methods. These findings demonstrate the potential of this method to enhance machining performance and contribute to the development of high-precision and high-efficiency machining processes for difficult-to-cut materials.

**Author Contributions:** Conceptualization, D.-T.N.; Data curation, T.-B.M.; Formal analysis, D.-T.N.; Funding acquisition, T.-T.L.; Investigation, T.-T.L.; Methodology, D.-T.N.; Project administration, T.-B.M.; Resources, T.-B.M.; Software, T.-T.L.; Supervision, D.-T.N.; Validation, D.-T.N.; Visualization, D.-T.N.; Writing—original draft, T.-B.M.; Writing—review & editing, D.-T.N., T.-B.M. All authors have read and agreed to the published version of the manuscript.

**Funding:** This work was supported by Vietnam Ministry of Education and Training (MOET) under grant number B2022-BKA-08.

**Acknowledgments:** This work was supported by the Vietnam Ministry of Education and Training (MOET) under grant number B2022-BKA-08.

**Conflicts of Interest:** The authors declare no conflict of interest.

## References

1. Irving, A.D.; Clarence, L.M.; Russell, F.H. *High Temperature Machining Methods*; Armed Services Technical Information Agency, Arlington Hall Station: Arlington, VA, USA, 1963.
2. Rajput, M. CFD Modelling of Hot Machining Operation. Ph.D. Thesis, National Institute of Technology Rourkela, Rourkela, Orissa, India, 2010.
3. Makwana, R.; Prajapati, H. Experimental Investigation on Effect of Machining Parameters on Surface Roughness in Thermally Assisted Turning of mild steel. In Proceedings of the International Conference on Multidisciplinary Research & Practice, Ahmedabad, India, 30 November 2014; Volume 1, pp. 488–489.
4. Harpreet, E.M.G.S.; Sharma, E. Analysis of Surface Roughness and Material Removal Rate in Dry and Thermal Assisted Machining of EN8 Steel. *Int. J. Eng. Sci. Res. Technol.* **2015**, *4*, 577–583.
5. Baili, M.; Wagner, V.; Dessein, G.; Sallaberry, J.; Lallement, D. An Experimental Investigation of Hot Machining with Induction to Improve Ti-5553 Machinability. *Appl. Mech. Mater.* **2011**, *62*, 67–76. [\[CrossRef\]](#)
6. Rahim, E.A.; Warap, N.; Mohid, Z. Thermal-assisted machining of nickel-based alloy. In *Superalloys*; IntechOpen: London, UK, 2015; pp. 3–29.
7. Pimenov, D.Y.; Mia, M.; Gupta, M.K.; Machado, R.A.; Pintaude, G.; Unune, D.R.; Khanna, N.; Khan, A.M.; Tomaz, I.; Wojciechowski, S.; et al. Resource saving by optimization and machining environments for sustainable manufacturing: A review and future prospects. *Renew. Sustain. Energy Rev.* **2022**, *166*, 112660. [\[CrossRef\]](#)
8. Barewar, S.D.; Kotwani, A.; Chougule, S.S.; Unune, D.R. Investigating a novel Ag/ZnO based hybrid nanofluid for sustainable machining of inconel 718 under nanofluid based minimum quantity lubrication. *J. Manuf. Process.* **2021**, *66*, 313–324. [\[CrossRef\]](#)
9. Unune, D.R.; Mali, H.S. Current status and applications of hybrid micro-machining processes: A review. *Proc. Inst. Mech. Eng. Part B J. Eng. Manuf.* **2014**, *229*, 1681–1693. [\[CrossRef\]](#)
10. Xavierarockiaraj, S.; Kuppan, P. Investigation of cutting forces, surface roughness and tool wear during Laser assisted machining of SKD11 Tool steel. *Procedia Eng.* **2014**, *97*, 1657–1666. [\[CrossRef\]](#)
11. Thi-Bich, M.; Van-Chien, D.; Tien-Long, B.; Duc-Toan, N. Cutting Force Model for Thermal-Assisted Machining of Tool Steel Based on the Taguchi Method. *Metals* **2018**, *8*, 992. [\[CrossRef\]](#)
12. Mac, T.-B.; Banh, T.-L.; Nguyen, D.-T. Study on cutting force and chip shrinkage coefficient during thermal-Assisted machining by induction heating of SKD11 steel. *J. Korean Soc. Precis. Eng.* **2019**, *36*, 803–811. [\[CrossRef\]](#)
13. Mac, T.-B.; Luyen, T.-T.; Nguyen, D.-T. A Study for Improved Prediction of the Cutting Force and Chip Shrinkage Coefficient during the SKD11 Alloy Steel Milling. *Machines* **2022**, *2022*, 229. [\[CrossRef\]](#)
14. Thanh-Huan, N.; Duc-Toan, N. Experimental Researches of Turning Hardened 9CrSi Alloy Tool Steel with Laser-Assisted Machining. *Arab. J. Sci. Eng.* **2021**, *46*, 11725–11738. [\[CrossRef\]](#)
15. Dong, T.P.; Toan, N.D. A study on the investigation of the microstructure of SKD61 steel after selected quenching and tempering processes. *Mod. Phys. Lett. B* **2023**, 2340022. [\[CrossRef\]](#)
16. Ginta, T.L.; Amin, A.K.M.N. Thermally-Assisted End Milling of Titanium Alloy Ti-6Al-4V Using Induction Heating. *Int. J. Mach. Mach. Mater.* **2013**, *14*, 194–212. [\[CrossRef\]](#)
17. Wang, Y.; Ding, C.; Tang, F.; Zheng, D.; Li, L.; Xie, S. Modeling and simulation of the high-speed milling of hardened steel SKD11 (62 HRC) based on SHPB technology. *Int. J. Mach. Tools Manuf.* **2016**, *108*, 13–26. [\[CrossRef\]](#)
18. Wang, Z.Y.; Rajurkar, K.P.; Fan, J.; Lei, S.; Shin, Y.C.; Petrescu, G. Hybrid machining of Inconel 718. *Int. J. Mach. Tools Manuf.* **2003**, *43*, 1391–1396. [\[CrossRef\]](#)
19. Dong, T.; Toan, N.; Dung, N. Influence of heat treatment process on the hardness and material structure of SKD61 tool steel. *Mod. Phys. Lett. B* **2023**, 2340014. [\[CrossRef\]](#)
20. Mruthunjaya, M.; Yogesh, K.B. A review on conventional and thermal assisted machining of titanium based alloy. *Mater. Today Proc.* **2021**, *46*, 8466–8472. [\[CrossRef\]](#)
21. Sun, S.; Brandt, M.; Dargusch, M.S. Thermally enhanced machining of hard-to-Machine materials—A review. *Int. J. Mach. Tools Manuf.* **2010**, *50*, 663–680. [\[CrossRef\]](#)
22. Maitya, K.; Swain, P. An experimental investigation of hot-machining to predict tool life. *J. Mater. Process. Technol.* **2008**, *198*, 344–349. [\[CrossRef\]](#)
23. Germain, G.; Lebrun, J.-L.; Robert, P.; Santo, P.; Poitou, A. Experimental and numerical approaches of laser assisted turning. *Int. J. Form. Process.* **2005**, *8*, 347–361.
24. Jeon, Y.; Pfefferkorn, F. Effect of laser preheating the workpiece on micro end milling of metals. *J. Manuf. Sci. Eng. Trans. ASME* **2008**, *130*, 1–9. [\[CrossRef\]](#)
25. Dumitrescu, P.; Koshy, P.; Stenekes, J.; Elbestawi, M. High-power diode laser assisted hard turning of AISI D2 tool steel. *Int. J. Mach. Tools. Manuf.* **2006**, *46*, 2009–2016. [\[CrossRef\]](#)
26. Kannatey-Asibu, E. *Principles of Laser Materials Processing*; John Wiley & Sons, Inc.: Hoboken, NJ, USA, 2009.
27. Wang, C.; Xie, Y.; Zheng, L.; Qin, Z.; Tang, D.; Song, Y. Research on the Chip Formation Mechanism during the high-speed milling of hardened steel. *Int. J. Mach. Tools Manuf.* **2014**, *79*, 31–48. [\[CrossRef\]](#)
28. Rudnev, V.; Love30less, D.; Cook, R.; Black, M. *Handbook of Induction Heating*; Marcel Dekker: New York, NY, USA, 2003.

- 
29. Thi-Hoa, P.; Thi-Bich, M.; Van-Canh, T.; Tien-Long, B.; Duc-Toan, N. A study on the cutting force and chip shrinkage coefficient in high-speed milling of A6061 aluminum alloy. *Int. J. Adv. Manuf. Technol.* **2017**, *98*, 177–188. [[CrossRef](#)]

**Disclaimer/Publisher's Note:** The statements, opinions and data contained in all publications are solely those of the individual author(s) and contributor(s) and not of MDPI and/or the editor(s). MDPI and/or the editor(s) disclaim responsibility for any injury to people or property resulting from any ideas, methods, instructions or products referred to in the content.